

University of Bristol  
Faculty of Engineering



Sensors, Signals and Control

---

## Part 2: Elevation Axis– Theory and Simulation with Control Requirements

---

*Supervisors:*  
**Andres Marcos**

*Email:*  
Andres.Marcos@bristol.ac.uk

*Authors:*  
**Alex Charles**  
**Akash Ramineni**

*Candidate Number:*  
(ac13625)  
(ar14120)

*7th April 2017*

## 1 P-I-D analysis

This report introduces the effects of proportional, derivative and integral gains, implemented by a conventional PID controller on a Quanser's behaviour<sup>a</sup>. This is assessed using time-domain and root locus results. A closed loop PID controller, is used to reduce tracking error ( $e$ ) between the control input and the observed output [1]. Through correctly tuning the PID controller, it is desirable to achieve a sharp response to a unit step input. The simulated results were verified by theory predictions.

### 1.1 Proportional Feedback Controller

Proportional gain control uses the *Present* state of a plant to error correct. The correction applied is proportional to the deviation from the desired state of the plant. The result causes a highly oscillatory system response, as the present error evaluates the instantaneous state of the plant only. The simulation shown in Figure 1 found the effect of varying proportional gain ( $K_p$ ) for the Quanser transfer function. The simulation executed an iterative loop with varying  $K_p$  from 0 to 0.1 in increments of 0.01. Figure 2 shows the time domain response of increasing  $K_p$ . When  $K_p = 0$ , a flat line was observed as there is no signal passing through the plant. By extending proportional gain, the correction factor became larger, increasing amplitude for higher  $K_p$  gains. The `stepinfo()` function revealed that an increase in  $K_p$ , reduced both rise time and steady-state error while raising overshoot.

The root locus plot in 3 allows observation of s-domain features with varying proportional gain. For pure variation in proportional gain, the (stable) poles are restricted to the same distance from the imaginary axis. By increasing  $K_p$  the poles moved away from the real axis in both directions, increasing natural-frequency ( $\omega_n$ ) and decreasing damping ratio  $\zeta$ . The result verifies the observation noted in the time domain response, as increased natural frequency will lead to greater oscillatory behaviour, and reduced damping ratio increases the overshoot.

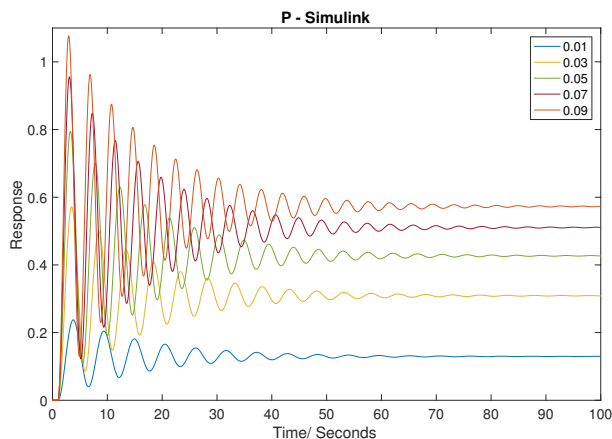


Figure 2: Response of Varying  $K_p$

### 1.2 Derivative Feedback Controller

Derivative control utilises the expected *Future* state of the system to preemptively correct the error signal,  $e$ . This correction is proportional to the

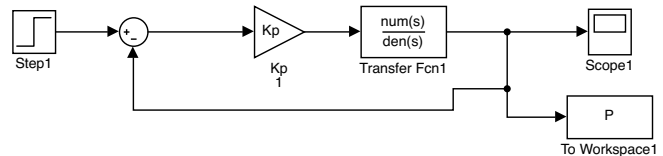


Figure 1: Proportional Feedback Controller

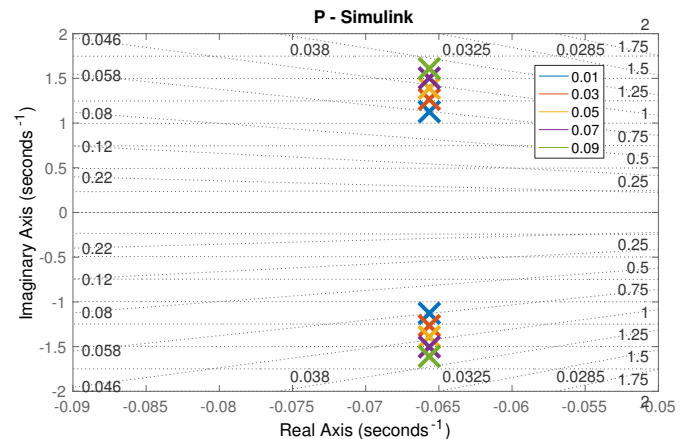


Figure 3: Poles of Varying  $K_p$

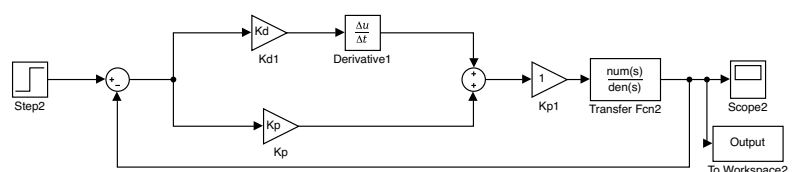


Figure 4: PD Feedback Controller

<sup>a</sup>See Control Coursework Part 1 for a derivation of the open-loop second order transfer functions for the Quanser elevation axis

rate of change of the system state at any one point in time. The system predict the future plant state based on the rate of change condition. It then accounts for the effects of this condition in the error response. For this reason, a large damping effect is expected for increasing derivative gain ( $K_d$ ). The simulation in Figure 4 was implemented to observe the effect of pure variation of  $K_d$  with constant a  $K_p$ . Figure 5 shows the effect of varying both gains by the same magnitude; controlled using an additional gain block after the controller. Gain values in Figure 5 and Figure 6 were incremented from 0 to 1 in increments of 0.1.

Both time domain responses show that increasing  $K_d$  has a greater damping effect on oscillations, reducing overshoot while increasing rise time. For a  $K_d = 0$ , large oscillations were observed, decreasing with higher gain values. For gain values of 0.6 and above, both high damping and quick settling times were observed. Increasing both  $K_d$  and  $K_p$  by the same amount shows a reduction in rise time, overshoot and steady-state error. The root locus S-domain metrics in Figure 7 show that as  $K_d$  increases the poles are shifted negatively in the real axis. The semi-circular shape represents the line of equal proportional gain, and the points represent varying  $K_d$  at that  $K_p$  level. As  $K_d$  is increased, the polar angle also increases. This implies poles closer to the real axis, (higher  $K_d$ ) correspond to poles with greater damping; the natural frequency is therefore reduced, decreasing oscillatory behaviour.

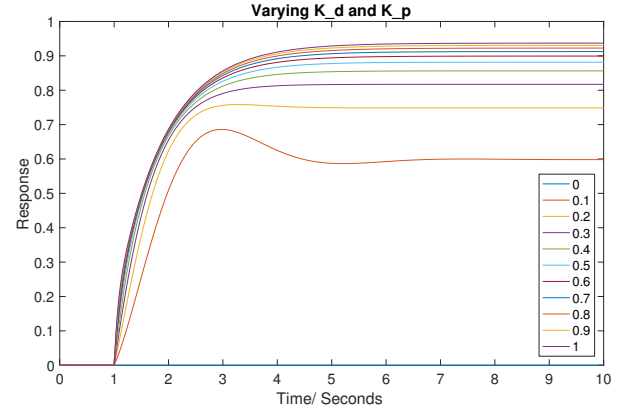


Figure 5: Time-Domain Response For Varying  $K_p$  and Varying  $K_d$

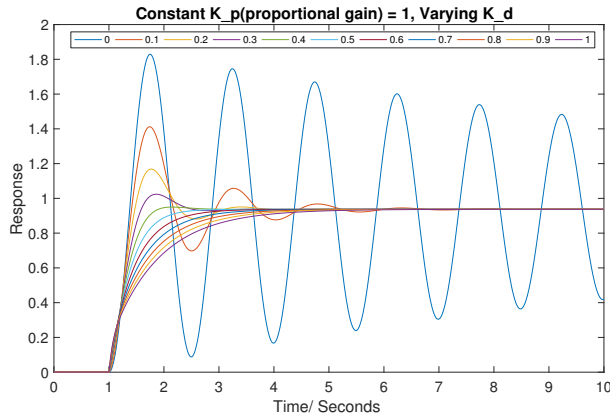


Figure 6: Time-Domain Response For Constant  $K_p$  and Varying  $K_d$

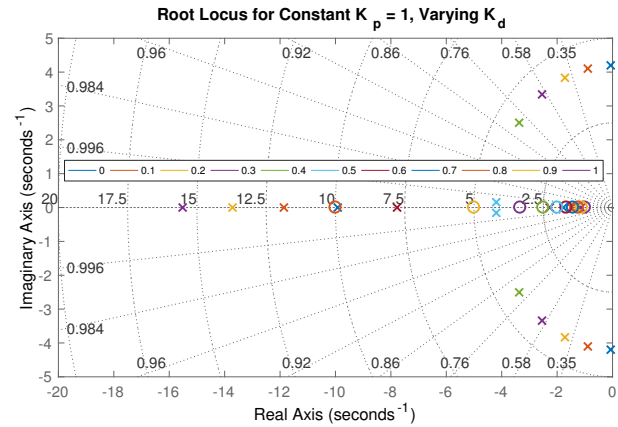


Figure 7: Poles of Constant  $K_p$  and Varying  $K_d$

### 1.3 Integral Action

Integral control utilises the Past state of the system to produce an error-correcting signal. The integral controller sums the historical tracking errors up to current time state, eliminating offset and leading to a zero steady-state error. The simulation of a full PID controller is shown in Figure 8. Figure 9 shows the variation of pure integral gain ( $K_i$ ) with constant  $K_p$  and  $K_d$ . Figure 11 shows the variation of all three gains  $K_d$ ,  $K_i$  and  $K_p$  by the same magnitude. This was implemented using a gain-scaling block placed after the controller. The time domain

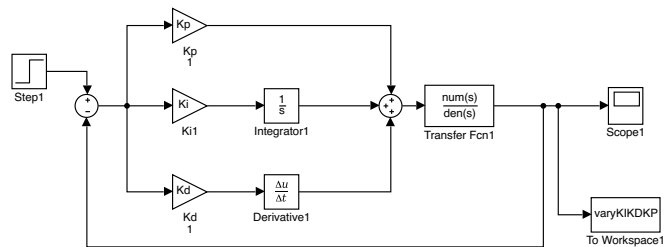


Figure 8: PID Feedback Controller

plots confirm the zero steady-state error as the oscillations settled at unity step input.

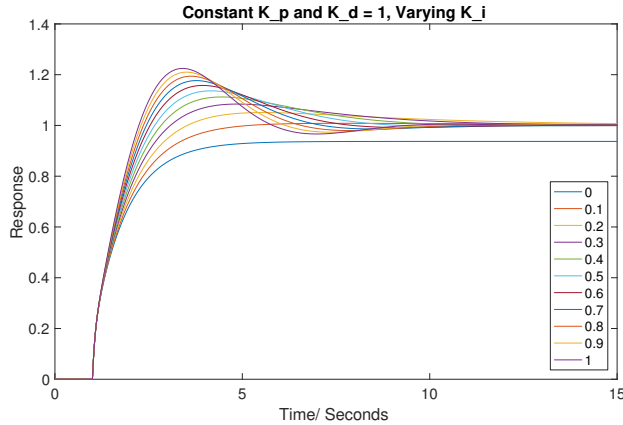


Figure 9: Time-Domain Response For Constant  $K_p$ ,  $K_d$  and Varying  $K_i$

At  $K_i = 0$  a large steady-state error exists in the system. However as  $K_i$  increases, the steady state error is reduced until it becomes negligible. The root locus plot in Figure 10, implies a stable system for the chosen gain range.

Observing the three controllers, for Quanser elevation, it is important to have a behaviour with a very low steady-state error and damped oscillations. This is due to a Quanser pilot requiring precise elevation, particularly at landing and taking off. Based on these requirements a PID controller appears to be the most appropriate feedback method for the Quanser's elevation response transfer function.

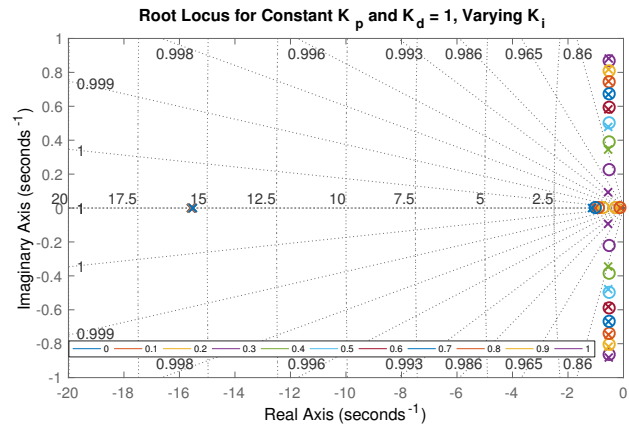


Figure 10: Poles of Constant  $K_p$ ,  $K_d$  and Varying  $K_i$

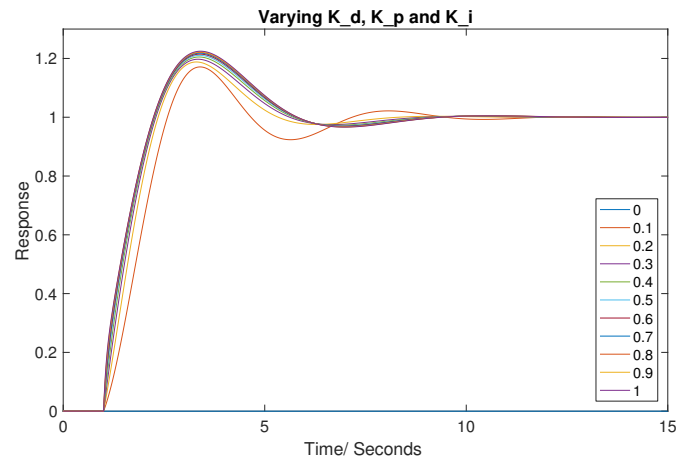


Figure 11: Time-Domain Response For Varying  $K_p$ ,  $K_d$  and  $K_i$

## 2 PID Design to Achieve Control Requirements

Through implementing the learning gained in part 1, a closed loop-feedback controller was then developed for the theoretical Quanser transfer functions (see below)<sup>b</sup>. This controller was tuned, through creating a script which produced the step response of the controller, displaying results using the `stepinfo()` function. Due to the steady state error response observed through using either a P or PD controller, it was decided to iterate different gains for using a full PID controller, to obtain the optimum response. Initially all gains were iterated using the gain-scaling block (discussed in section 1.3). Through observing the different responses, a rough estimate was found for all three gains, which could then be individually tweaked based on the parameters shown in Table 1. Results were also refined using Matlab's inbuilt PID tuner, helping rise and settling time objectives.

Table 1: Effect of Increasing PID Gains on Objectives

	Objectives			
	Tr	Ts	%OS	Ess
<b>Kp</b>	Decrease	Small Increase	Increase	Decrease
<b>Kd</b>	Small Change	Decrease	Decrease	Small Change
<b>Ki</b>	Decrease	Increase	Increase	Eliminate

<sup>b</sup>The first order transfer function obtained in Control part 1, was corrected using the  $\tau$ .  $\tau = \zeta \times \omega_n$

$$2^{nd} \text{ Order: } k \cdot \frac{1.109 \cdot \frac{180}{\pi}}{s^2 + 0.1313s + 1.109}$$

$$1^{st} \text{ Order: } k \cdot \frac{1}{15.24s + 1}$$

## 2.1 PID Controller Tuning

As the proportional, integral and derivative gain values were adjusted to tune the PID, the characteristics for changing each gain were considered with reference to Table 1. The controller was then tuned as necessary to best meet the requirements. Analysing the first order transfer function response, a high rise and settling time were both observed. As the Quanser behaves as a second order system, it was decided to neglected the first order transfer function in favour of the second order transfer function. The tuned response can be seen in Figure 12.

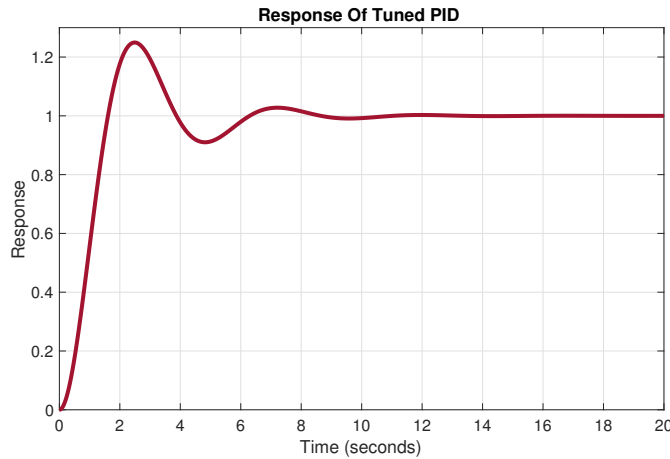


Figure 12: Tuned PID Response

Table 2: Tuned PID Transfer Function Values

		Task	Tuned PID
Objectives	Tr (s)	12	0.76
	Ts (s)	10	4.6387
	OS (%)	20	5.211
	Ess (%)	5	0.3
Selected Gain Values			
Kp = 0.1, Kd = 0.1, Ki = 0.1			

## 2.2 Tuned Quanser Controller

A PID controller with the stated  $K_p$ ,  $K_d$ , and  $K_i$  values was created inside the SSC17\_QuanserPart2\_PID design.slx controller block. The second order transfer function was placed into the empty PLANT block. The expected Quanser response then observed for the chosen PID and plant configurations. In addition the two other EXTREME plants were tested to ensure the controller was working effectively. Figure 13 shows the design configuration response due to step input as well as the extreme plant response to the designed controller.

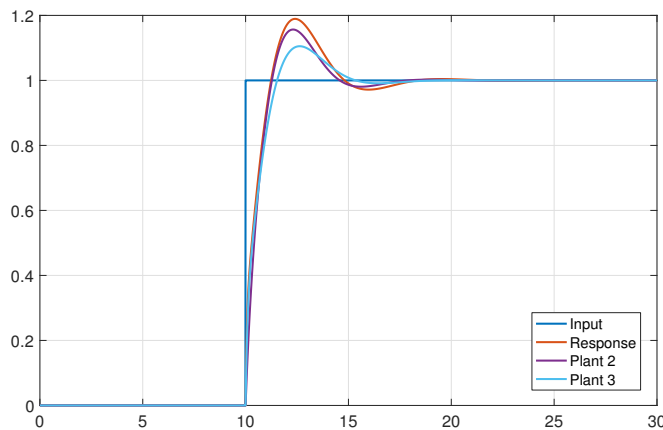


Figure 13: Expected Quanser Response of PID Controller

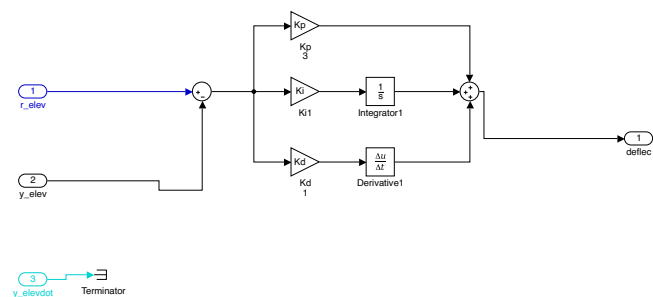


Figure 14: Simulation Used for Theory Controller

## References

- [1] (2012). Introduction: pid controller design, [Online]. Available: <http://ctms.engin.umich.edu/CTMS/index.php?example=Introduction&section=ControlPID> (visited on 07/04/2017).